# Comparation of the structural characteristics and biological activities of chondroitin sulfates extracted from notochord and backbone of Chinese sturgeon *(Acipenser sinensis)*

Dawei Meng[a,b]*, Xiaoqian Leng[a], Yan Zhang[c], Jiang Luo[a], Hao Du[a], Yasuaki Takagi[d], Zhiyuan Dai[b], Qiwei Wei[a]*

*a Key Laboratory of Freshwater Biodiversity Conservation, Ministry of Agriculture and Rural Affairs, Yangtze River Fisheries Research Institute, Chinese academy of Fishery Sciences, Wuhan, 430223, China*

*b Zhejiang Province Joint Key Laboratory of Aquatic Products Processing, Institute of Seafood, Zhejiang Gongshang University, 149 JiaoGong Road, Hangzhou 311112, China*

*c Liangzhu laboratory, Zhejiang University Medical Center, Hangzhou 310058, Zhejiang, China*

*d Faculty of Fisheries Sciences, Hokkaido University, 3-1-1 Minato-cho, Hakodate, Hokkaido 041-8611, Japan*

Corresponding author:

1. Zhejiang Province Joint Key Laboratory of Aquatic Products Processing, Institute of Seafood, Zhejiang Gongshang University, Hangzhou 310012, China.

2. Key Laboratory of Freshwater Biodiversity Conservation, Ministry of Agriculture and Rural Affairs, Yangtze River Fisheries Research Institute, Chinese academy of Fishery Sciences, Wuhan, 430223, China

E-mail addresses:

dawei@mail.zjgsu.edu.cn (D. Meng), lengxiaoqian123@126.com (X. Leng), 913241136@qq.com (Y.

Zhang), 815374384@qq.com (J. Luo), duhao@yfi.ac.cn (H. Du), takagi@fish.hokudai.ac.jp (Y. Takagi), dzy@zjgsu.edu.cn (Z. Dai), weiqw@yfi.ac.cn (Q. Wei).

**Abstract**

To compare the structural properties and biological activities of chondroitin sulfate (CS) in two different tissues of Chinese sturgeon *(Acipenser sinensis)* and Russian sturgeon *(Acipenser gueldenstaedti)*, we extracted their backbone cartilage CS (Cart-CS) and notochord CS (Noto-CS), and analyzed the CS structural properties using chromatographic and spectroscopic methods. The molecular weights of Chinese sturgeon Cart-CS and Noto-CS were 54.7 and 25.4 kDa, respectively, and the molecular weights of Russian sturgeon were 50.0 and 38.4 kDa, respectively. The disaccharide composition results showed that Cart-CS was mainly composed of CS-C, while Noto-CS was almost composed of pure CS-A. The antioxidant activity of sturgeon CS and its effect on collagen fibril formation were discussed. Sturgeon CS exhibited higher antioxidant activity than shark and bovine CSs. Sturgeon CS inhibited the self-assemble of type I collagen into fibrils. The inhibition effect of Cart-CS was higher than that of Noto-CS. The high value-added utilization of Cart-CS and Noto-CS will increase the value of sturgeon by-products. Furthermore, the disaccharide composition of CS in sturgeon depends on tissues of origin, but not on species. It means that the CS of Chinese sturgeon can be substituted by the CS of other commercial sturgeon. That will contribute to the protection of endangered species of Chinese sturgeon from illegal fishing and increase the value of commercial sturgeon by-products.

**Keywords**

Chinese sturgeon; Russian sturgeon; Chondroitin sulfate; Structure properties; Antioxidant activity; Collagen fibril

## 1. Introduction

Chinese sturgeon (*Acipenser sciensis*) is an ancient fish that dates back 1.4 million years ago. It inhabits mainly in the East China sea and Yangtze River basin in China [1]. Due to overfishing and destruction of the living environment in Yangtze River, the Chinese sturgeon population has dropped from more than 10,000 individuals in the 1970s to less than 57 individuals in 2010 [2]. Since 1988, the International Union for Conservation of Nature (IUCN) now has listed Chinese sturgeon as critically endangered and protected species since 1988 [3] and the Convention on International Trade in Endangered Species of Wild Fauna and Flora (CITES) has listed Chinese sturgeon under Appendix II [4]. According to the Chinese law, wild Chinese sturgeon is a national first-class protected animal [5]. In order to avoid Chinese sturgeon from extinction, artificial breeding technology has been successfully explored in the past 15 years and the number of farmed Chinese sturgeon has increased remarkably [6].

From ancient China, Chinese sturgeon has been used as an edible fish. According to the records in the Compendium of Materia Medica, it is considered that its consumption can cure scabies and invigorate the spleen and lungs but unauthorized fishing as well as commercial use of artificially bred Chinese sturgeon is illegal at present in China. Thus, medical functionalities of the Chinese sturgeon are unusable treasures at present. Furthermore, so far, little research has been done on the structural properties of functional substances of this ancient fish. Therefore, the study on the structural characteristics and functions of biologically active substances contained in Chinese sturgeon will promote the discovery of its functional mechanisms. Meanwhile, it will help to find the functional substitutes from other available resources, thereby protecting the endangered species of Chinese sturgeon from illegal fishing.

Russian sturgeon *(Acipenser gueldenstaedti)* is native to the Caspian Sea, the Black Sea, and the

Azov Sea [7] and is a commercial sturgeon species accounting for 10% of the annual production of sturgeon in China [8]. The main purpose of Russian sturgeon farming is the production of caviar. Because of the long farming period required to obtain caviar. Russian sturgeon is more expensive to farm than other fishes, including hybrid sturgeons. The lack of efficient use of sturgeon tissues other than caviar constrains the profitability of aquaculture industry and leads to waste of fish sources. Cartilage and notochord, which contain high amounts of chondroitin sulfate (CS) and type II collagen, are the two main by-products of sturgeon processing. If these CS and type II collagen sources can be developed into highly value-added commercial products, their economic benefits will support the further development of the sturgeon farming industry. Meanwhile, it will also reduce the waste of aquatic resources. In previous studies, we have deeply explored the extraction method and biochemistry characteristics of sturgeon notochord type II collagen [9]. The structural properties of the sturgeon CS have not been addressed in our study. In recent study, Shionoya reported the structural properties of CS derived from the head cartilage of Russian sturgeon [10]. However, there was no study on the extraction and the structural properties of Russian sturgeon notochord and backbone cartilage CS.

CS is a linear natural biological macromolecule contained in the connective tissues of practically all animal origins [11]. In the human body, CS contributes the structural function of extracellular matrix and plays an important role in wound healing, promotion of neurite outgrowth, regulation of the growth factors, cell adhesion, and cell division [12, 13]. The linear polysaccharides chain of CS consists of alternating disaccharide units of glucuronic acid and N-acetyl-galactosamine linked by β (1-3) and β (1-4) glycosidic bonds and modified with sulfated groups [14]. According to the degree and position of sulfated groups on the polysaccharide chain, CSs are classified into several types. In the organisms,

CS-A and CS-C are the two most common types, in which the mono-sulfated group is located at the C-4 and C-6 of the N-acetyl-galactosamine, respectively [15]. The CS extracted from animal tissues showed various biological activities *in vitro*, such as anticoagulant, anti-inflammatory and antioxidant activities [16-19]. It is widely used as a healthy functional supplements and medicine, especially for joint diseases, such as osteoarthritis [16, 17]. The bioactivity of CS is directly related to its structure characteristics. For example, in human cartilage, CS-A seems to be involved in the ossification process, whereas CS-C is involved in the integrity of articular surfaces [20]. Rachmilewitz reported that CS-A could activate peripheral blood mononuclear cell types and activate monocytes, whereas CS-C did not play these functional roles [21]. The *in vitro* antioxidant activity of CS-A is higher than that of CS-C because of its strong metal cation binding capacity [19]. In addition, as the main components of extracellular matrix, CS and collagen are often used as biomaterials due to their structural and functional properties [22]. However, most of the CS and collagen used in biomaterials are derived from mammalian tissues, and less research has been done on fish-derived CS and collagen. The outbreaks of zoonosis, such as BSA and FMD, and religious beliefs limit the use of mammalian materials now [23]. The application in the field of biomedical materials will greatly enhance the value of sturgeon CS and collagen.

The objective of this study is to elucidate the structural properties of CS in Chinese and Russian sturgeon. By comparing the structure properties and antioxidant activity of CS, we demonstrate that the functional substances of Chinese sturgeon can be substituted by those of other edible sturgeon, thereby helping to reduce the illegal fishing and utilization of endangered Chinese sturgeon. Meanwhile, it will increase the value of the by-products of farmed Russian sturgeon. Firstly, we purified the CSs from backbone cartilage and notochord of farmed Chinese sturgeon and Russian sturgeon, respectively.

Secondly, we analyzed and compared the structural characteristics of CS by chromatographic and spectroscopic technologies. Thirdly, we detected the antioxidant activity of sturgeon CS using ABTS and hydroxyl radical scavenging assays. Finally, we investigated the effect of sturgeon CS on type I collagen fibril formation.

## 2. Materials and methods

### 2.1 Materials

The backbone cartilage and notochord of farmed Chinese sturgeon (*Acipenser sinensis*) were procured from the Key Laboratory of Freshwater Biodiversity Conservation and the Key Laboratory of Freshwater Biodiversity Conservation, Yangtze River Fisheries Research Institute, Hubei, China. The farmed Chinese sturgeon used in this study was the second generation for scientific research. Chinese sturgeon handling and experimental procedures used in this study were approved by the Animal Care and Use Committee of the Yangtze River Fisheries Research Institute, Chinese Academy of Fishery Sciences. The backbone cartilage and notochord of Russian sturgeon were obtained from the Sturgeon Biological Technology Co. Ltd. (Xinchang county, Zhejiang province, China). The materials were kept in dry ice to be transported to the laboratory. The internal semisolid of notochord tube and the flesh on the surface of backbone cartilage were removed. Then, notochord sheath and backbone cartilage were lyophilized in a freeze dryer (FreeZone 2.5 L, American Labconco Co., Ltd., Kansas City, USA). The dry samples were stored at -30 °C until use.

### 2.2 Extraction of CSs

Backbone cartilage fat was removed over 24 h in anhydrous ethanol (two solution-changes) at 4 °C with a sample: solution ratio of 1:10 (w/v). Defatted cartilage and notochord were cut into small pieces (approximately 0.2 × 0.2 cm) for CS extraction. Two tissues were continuously stirred in a

133 solution of 0.1 M NaOH for 24 h at 4 °C, with a sample: solution ratio of 1: 50 (dry w/v; two solution-
134 changes). After alkaline treatment, the mixtures were centrifuged at 10,000 ×g for 30 min at 4 °C
135 (Sorvall LYNX4000., Thermo fisher scientific., Waltham, USA). The supernatant was neutralized to
136 pH 8.0 with dilute HCl. Enzymatic hydrolysis was achieved by the addition of papain (EC 3.4.23.1,
137 1:10,000., Solarbio Science & Technology Co, Ltd., BeiJing., China) with a ratio of papain: solution
138 1:5000 (w/v, g/mL). The reaction was kept for 4 h at 50 °C with a stirring. After enzymatic hydrolysis,
139 the reaction was terminated by boiling samples for 10 min. The crude CS was precipitated with 3
140 volumes of anhydrous ethanol at 4 °C overnight, and then collected by centrifugation at 10,000 g for 30
141 min. The precipitate was dissolved in 20 mM Tris-HCl buffer (pH 8.0) containing 50 mM NaCl. The
142 solution was applied to a column (1.5 cm × 7 cm) packed with UNOsphere Q strong anion-exchange
143 media (Bio-Rad Laboratories, Inc., Hercules, CA, USA) and equilibrated in 20 mM Tris-HCl and 50
144 mM NaCl. The crude CS was eluted with a linear gradient of NaCl (50 mM to 2 M in 90 min) in 20
145 mM Tris-HCl using Biologic LP system (Bio-Rad Laboratories, Inc, Hercules, CA, USA) at flow rate
146 of 1 mL/min. The eluate solution was collected in each 5 min. Three volumes of ethanol were added
147 into collection tube to purify CS. The precipitate was collected and re-dissolved in deionized water, and
148 then dialyzed against 50 times volume of deionized water (two solution-changes) using a 200-Da
149 dialysis membrane to remove NaCl. Finally, the dialysis fluid was lyophilized and stored at -30 °C until
150 used. The percentage of dry weight of CS extracted in comparison with the dry wight of the initial
151 tissues was calculated as the CS yield.

152 **2.3. Molecular weight distribution**

153 The average molecular weight of CS was analyzed by Gel permeation chromatography/size-
154 exclusion chromatography (GPC/SEC). An Agilent 1260 Infinity II Multi-detector GPC/SEC system

(Agilient Technologies., CA, USA) was coupled with a refractive index detector and a multi-angle laser light scattering (Wyatt Dawn Heleos-II., USA). Separation was performed using a Agilent PL aquagel-OH Mixed-H column (8 μm, 7.5 mm × 300 mm) and was eluted with 0.1 M $NaNO_3$ at 1.0 mL/min (45 °C). The CS was prepared at a concentration of 1 mg/mL using mobile phase and the injection volume was 50 μL. The average molecular weight calculations were performed by Agilent GPC/SEC software (Agilient Technologies, CA, USA).

**2.4. UV spectroscopic analysis**

The CS samples were prepared as a 1 mg/mL solution with deionized water. The UV spectra were recorded in the wavelength range from 190 to 500 nm (Evolution 60 s., Thermo fisher scientific., Waltham, USA). Deionized water was used instead of the sample solution as control measurement. Each measurement was replicated three times.

**2.5. Infra-red spectroscopic analysis**

The Infra-red spectra of CS were recorded with an infrared spectrophotometer (Nicolet iS10., Thermo Scientific., Madison, USA). The CS powder was ground together with potassium bromide (w/w 1:200), and then pressed into a 1 mm pellet for measurement in the spectra range of 500-4000 $cm^{-1}$. The potassium bromide powder was used as the background. Each measurement was replicated three times.

**2.6. $^1$H NMR spectroscopic analysis**

The $^1$H-NMR spectra of CS were recorded using a Bruker Avance 600 (Karl-scrube., Germany) operating at 600 MHz. The lyophilized sample was dissolved in $D_2O$ at a 10 mg/mL concentration and the spectra were recorded at 298 K. The $^1$H chemical shifts (d, ppm) were quoted with respect to external sodium 4, 4-dimethyl-4-silapentane-1-sulfonate (0.0 ppm). Each measurement was replicated

three times.

**2.7. Disaccharide composition**

Disaccharide analysis was performed according to the method of Maccari [24] with minor modifications. CS was dissolved in Tris-acetate buffer (50 mM Tris and 60 mM of sodium acetate, pH 8.0) to 10 mg/mL. Eighty microliter chondroitinase ABC (6mU/μL, EC 4.2.2.4, Sigma-Aldrich., Saint louis., USA) was mixed into 400 μL CS solution. The reaction was performed for 24 h at 37 °C. Then, the mixture was boiled for 10 min to terminate reaction and filtered through 0.22 μm syringe filters. The solution was fractionated by ultrafiltration using molecular weight cutoff of 3 kDa (Merck Millipore Ltd., Darmstadt., Germany). The fraction of molecule weight below 3 kDa was collected for analysis of disaccharide composition. The disaccharide sample was detected by HPLC with Waters 2695 Pump system, Waters 2489 UV/Vis detector (Waters Co., USA) and a Spherisorb SAX column (4.6 mm × 150 mm, 5 μL, Waters Co., USA), with a linear gradient from 5 to 35 min using 0 to 1 M NaCl (pH 3.5) solution as mobile phase. The absorbance was monitored at 232 nm. Shark cartilage CS (Sigma-Aldrich., Saint louis., USA) was used as standard and was analyzed by the same method. Each experiment was replicated three times.

**2.8. Antioxidant activity analysis**

**2.8.1 ABTS scavenging activity**

The ABTS radical scavenging activity was determined by the method of Li et al. [25]. In brief, ABTS radical cation was generated by mixing the ABTS stock solution (7 mM) with potassium persulfate (2.45 mM). The mixture was left in the dark at room temperature for 16 h. The ABTS radical solution was diluted in 5 mM phosphate buffered saline at pH 7.4 to an absorbance of 0.7 at 734 nm. One milliliter of diluted ABTS radical solution was mixed with 1 ml of different concentrations of

199 samples. Ten minutes later, the absorbance was measured at 734 nm against the corresponding blank.
200 Vitamin C (Vc) was used as positive control. The ABTS radical scavenging activity of samples was
201 calculated according to Eq. 1:
202 Scavenging activity (%) = [ (Ac – As) / Ac ] × 100%
203 where As and Ac are the absorbances with and without a sample.
204 **2.8.2. Hydroxyl scavenging activity**
205 Hydroxyl radical scavenging activity was determined according to the method of Pan et al. [26].
206 Briefly, a 1,10-phenanthroline solution (1.0 ml, 1.865 mM) was mixed with 2 ml of the sample
207 solution, and then $FeSO_4 \cdot 7H_2O$ solution (1.0 ml, 0.75 mM) was pipetted into the mixture. The reaction
208 was initiated by adding 1.0 ml of $H_2O_2$ (0.01% v/v). After incubation at 37°C for 60 min, the
209 absorbance was measured at 536 nm against a reagent blank. The reaction solution without antioxidants
210 was used as a negative control, and the mixture without $H_2O_2$ was used as the blank. Vc was used as
211 positive control. The hydroxyl radical scavenging activity was calculated according to Eq. 2:
212 Scavenging activity (%) ＝ [ (As – An) / ( Ab – An) ] × 100%
213 where As, An, and Ab are the absorbance values at 536 nm of the sample, negative control, and blank
214 after the reaction, respectively.
215 **2.9. The effects of CS on type I collagen fibril formation**
216 **2.9.1. Fibril formation**
217 Sturgeon skin pepsin-soluble type I collagen was extracted according to the method of Meng et al.
218 [9]. The fibril formation process of type I collagen was evaluated by the method of Meng et al. [27].
219 Lyophilized collagen was dissolved in pH 2.0 HCl solution to 3mg/mL. CS was added to Na-phosphate
220 buffer (60 mM, pH 7.4) at concentrations of 0 and 1.5 mg/mL, respectively. The collagen solution was

mixed with a Na-phosphate buffer with a ratio of 1:2 (v/v). After mixing, the mass ratio of CS to collagen were 0:1 and 1:1, respectively. The mixed solution was placed into a quartz cuvette, and the subsequent fibril formation at 21°C, for 30 min was monitored by measuring increased turbidity via optical absorbance at 340 nm, using a spectral monitor (Evolution 60 s., Thermo fisher scientific., Waltham, USA).

#### 2.9.2. Fibril morphology

The microstructure of collagen fibrils was observed using a scanning electron microscope (SEM; Sigma 500, Carl Zeiss Ltd, Germany). The collagen fibrils were formed and obtained by centrifugation at 10,000 ×*g* for 20 min at 4 ℃. The precipitated fibrils were fixed with 2.5% (v/v) glutaraldehyde in 60 mM Na-phosphate buffer (pH 7.4) for 1 h at room temperature, rinsed with Na-phosphate buffer to remove the fixative, dehydrated using a graded series of ethanol solutions, and soaked in a t-butyl alcohol solution for two 30-min intervals. Finally, the samples were freeze-dried in a t-butyl alcohol solution using a freeze-drying device and coated with gold-platinum, using an auto fine coater (JFC-1600; JEOL Ltd, Japan).

## 3. Results and discussion

### 3.1. The yield of CSs

The yields of backbone cartilage CS (Cart-CS) and notochord CS (Noto-CS) from Chinese sturgeon were 8.48 % and 10.47% (dry weight basis), respectively, and those from Russian sturgeon were 9.44% and 9.02% (dry weight basis), respectively. Gui et al reported that the yield of CS from hybrid sturgeon backbone cartilage was 22% [28]. Wang reported that the yield of CS from sturgeon (*Acipenser schrenckii*) cartilage was 25% [29]. In this study, the yields of CSs in Chinese and Russian sturgeon were lower than that of other sturgeon species. Fish species and age might be the reason for

differences in CS yield. In addition, different extraction methods could also lead to differences in CS yields. For example, Gui and Im et al. (2010) only used ethanol precipitation method to purify sturgeon backbone CS [28, 30]. In this research, in order to obtain pure CS for accurate analysis of structure properties, after ethanol precipitation process, we purified crude CS using ion-exchange chromatography. The losses in this process may be the reason for the lower yield than other studies.

Comparing with other fish species, the yields of Chinese and Russian sturgeon CS were higher than that from smooth hound cartilage CS (2.52%) [31], *Holothutis scabra* cartilage CS (2.89%) [32]. Because most of the researches only discussed the structural and biological properties of the notochord in fish body, but the studies on notochord utilization were scarce [33, 34]. To our know, only two studies discussed the structural and antigenic properties of the sturgeon Noto-CS, but no extraction method and yield data were mentioned [35, 36]. It was difficult to compare the yield of sturgeon Noto-CS with other notochordal tissues. The backbone cartilage and notochord occupy ca. 5.9% and 1.7% (wet weight basis) of the whole sturgeon body weight and the moisture contents of cartilage and notochord were ca. 60.4 % and 81.9% (data from the present research material). In 2017, the breeding volume of farmed sturgeon exceeded 8,000 tons in China [37]. It can be predicted that backbone cartilage and notochord of farmed sturgeon could provide more than 40 tons CS per year. Due to the abundant aquaculture resources in China, the sturgeon backbone and notochord have huge potential for large-scale production as new fish source CS.

### 3.2. Molecular weight of CSs

The average molecular weight (Mw) of CS was analyzed by GPC system and the result was shown in Fig. 1 and Table 1. All of four CSs exhibited a signal peak in the GPC-RI-MALLS chromatogram. It suggested that the CS samples have been purified. The average Mw of Cart-CS and

Noto-CS from Chinese sturgeon were 54.7 and 25.4 kDa; from Russian sturgeon were 50.0 and 38.4 kDa, respectively. The Mw of Cart-CS was higher than that of Noto-CS in both two sturgeons. It was the first time to compare the Mw of sturgeon Cart-CS and Noto-CS. Previous studies showed that the Mw of backbone cartilage CS from hybrid sturgeon *(Acipenser baerii* × *Acipenser schrenckii*) was 49.2 kDa [28]. The Mw of backbone cartilage CS from hybrid sturgeon (*Huso dauricus* × *Acipenser schrenckii*) was 32.6 kDa [38]. The Mw of CSs from Chinese and Russian sturgeons was similar to that of other hybrid sturgeon cartilage CSs. The Mw of Chinese sturgeon Cart-CS was higher than Mw of bovine cartilage CS (34.4 kDa), while lower than Mw of shark cartilage CS (75.8 kDa) [39]. It was difficult to compare the Mw of sturgeon Noto-CS with CSs from other notochordal tissues, because few studies have reported the Mw of notochordal CS.

### 3.3. UV spectra of CSs

The ultraviolet absorption of CS was identified using ultraviolet-visible spectrophotometer in the wavelength range from 190 to 500 nm, as shown in Fig. 2. All CSs exhibited similar absorption ranges from 190 to 220 nm, with a maximum absorbance peak at ranges from 199 to 206 nm. It was the characteristic absorption range of polysaccharides [31, 40]. Subtle differences might be due to the reduced sensitivity of spectrometer at low wavelengths. There had no apparent absorption at 260 nm and 280 nm, indicating that the nucleic acids and proteins were not mixed in CSs [40].

### 3.4. Infra-red spectra of CSs

The structure characteristics of CSs were analyzed by Infrared spectroscopy (Fig. 3 and Table 2). The spectral bands of CSs appeared in two ranges, 500 to 1800 $cm^{-1}$ and 3000 to 4000 $cm^{-1}$. The infrared spectroscopy of CSs were similar between sturgeon species, but were different between two tissues. The region of absorbance that clearly differed between Cart-CSs and Noto-CSs was from 800

to 900 $cm^{-1}$. In this region, the Cart-CS of Chinese sturgeon and Russian sturgeon exhibited two absorbance peaks at 825.87 and 853.35 $cm^{-1}$, 822.01 and 855.76 $cm^{-1}$, respectively. The Noto-CS of Chinese sturgeon and Russian sturgeon had only one strong absorbance peak at 856.51 $cm^{-1}$ and 856.59 $cm^{-1}$, respectively. Garnjanagoonchorn reported that the absorption in both the C-O-S axial and equatorial orientations of CS-A exhibited the special peak at 854.5 $cm^{-1}$, while CS-C exhibited the special peak at 823.7 $cm^{-1}$ [41]. It indicated that Cart-CS contained both CS-A and CS-C in the polysaccharide chain, but the main type of Noto-CS was CS-A. Furthermore, the peaks observed at 1071.3 $cm^{-1}$ and 1054.4 $cm^{-1}$ of Chinese sturgeon Cart-CS and Noto-CS; at 1073.2 $cm^{-1}$ and 1052.0 $cm^{-1}$ of Russian sturgeon Cart-CS and Noto-CS were attributed to the C-C, C-O-C, C-OH ring vibrations [42]. The peaks detected at 1229.9 $cm^{-1}$ and 1236.2 $cm^{-1}$ of Chinese sturgeon Cart-CS and Noto-CS; at 1246.3 $cm^{-1}$ and 1235.7 $cm^{-1}$ of Russian sturgeon Cart-CS and Noto-CS were characteristics of S=O asymmetric stretching vibration [43]. The peaks detected at 1410.2 $cm^{-1}$ and 1415.0 $cm^{-1}$ of Chinese sturgeon Cart-CS and Noto-CS; at 1413.6 $cm^{-1}$ and 1417.0 $cm^{-1}$ of Russian sturgeon Cart-CS and Noto-CS were characteristics of C-O stretching [44]. The peaks detected at 1637.3 $cm^{-1}$ and 1636.3 $cm^{-1}$ of Chinese sturgeon Cart-CS and Noto-CS; at 1637.3 $cm^{-1}$ and 1639.7 $cm^{-1}$ of Russian sturgeon Cart-CS and Noto-CS were represented -$CONH_2$ structure [42]. The peak observed around 2922.1 $cm^{-1}$ and 2922.6 $cm^{-1}$ of Chinese sturgeon Cart-CS and Noto-CS; around 2926.0 $cm^{-1}$ and 2922.6 $cm^{-1}$ of Russian sturgeon Cart-CS and Noto-CS were attributed to the stretching vibration of C-H [44]. The strong absorbance peaks at 3415.3 $cm^{-1}$ and 3416.3 $cm^{-1}$ of Chinese sturgeon Cart-CS and Noto-CS; at 3422.6 $cm^{-1}$ and 3417.7 $cm^{-1}$ of Russian sturgeon Cart-CS and Noto-CS indicated the stretching of -OH [42, 44]. These results showed that except for the absorption of the C-O-S, the infrared spectroscopy of four CSs were almost same. It meant that the structure properties that differed among four CSs was the

sulfate pattern on the polysaccharide chain.

### 3.5. $^{1}$H-NMR spectroscopy of CSs

The $^{1}$H-NMR spectra of four CSs were shown in Fig. 4. All proton signals of CSs appeared in two spectral regions, one between 2.0 and 2.1 ppm, and the other between 3.0 and 5.0 ppm. It was the characteristic absorption area of CS [45]. No signal appeared between 2.0 to 3.0 ppm indicated that high purity CS was obtained [45]. The proton signal properties of the two Cart-CSs and the two Noto-CSs were almost identical. It suggested that the structural properties of CS were identical between the same tissue of two sturgeons. The significant differences between Cart-CS and Noto-CS appeared at 4.17 and 4.80 ppm. The Cart-CS had a strong signal peak at 4.17 ppm and a weak signal peak at 4.80 ppm. The Noto-CS only had a strong signal peak at 4.80 ppm. The characteristic signals at 4.17 and 4.80 ppm were assigned to H6 of GalNAc-6$SO_4$ and H4 of GalNAc-4$SO_4$, respectively [45, 46]. It indicated that polysaccharide structure of two Cart-CSs contained both CS-A and CS-C, and CS-C was the predominant sulfate pattern on the chain. The prominent signal at 4.80 ppm was detected in Noto-CS indicated that the sulfate pattern of both two Noto-CSs was CS-A. This result was consistent with the results of infra-red spectra described in Section 3.4. Furthermore, the peak between 1.9 to 2.1 ppm was the signal of acetyl methyl group proton [47]. The signals at 3.74, 3.98 and 4.14 ppm were assigned to H6, H2 and H4 of N-acetyl-galactosamine, while the signals at 3.32, 3.54 and 3.69 ppm were assigned to H2, H3 and H4/5 of glucuronic acid, respectively [47].

### 3.6. Disaccharide composition of CSs

To further investigate the disaccharide composition of four CSs, we hydrolyzed the CS with chondroitinase ABC and analyzed the disaccharide structure using SAX-HPLC, as shown in Fig. 5 and Table 1. The disaccharide composition of sturgeon CSs were analyzed by comparison with shark

cartilage CS and bovine cartilage CS. Shark Cart-CS consisted of non-sulfated disaccharide CS-0 (2.79%), and mono-sulfated disaccharide CS-A (28.91%) and CS-C (50.46%), and di-sulfated disaccharide CS-D (17.85%). Bovine Cart-CS consisted of non-sulfated disaccharide CS-0 (5.70%), and mono-sulfated disaccharide CS-A (63.79%) and CS-C (30.51%). This disaccharide composition was consistent with the previous report [39].

Sturgeon CSs were mainly composed of CS-0, CS-A, and CS-C in different proportions. The di-sulfated disaccharides were not detected in either sturgeon CS. The disaccharide composition of Chinese sturgeon Cart-CS was CS-0 (10.21%), CS-A (31.12%), and CS-C (58.67%), and the disaccharide composition of Russian sturgeon Cart-CS was CS-0 (6.79%), CS-A (37.70%), and CS-C (55.51%). The disaccharide composition of Chinese sturgeon Noto-CS was CS-0 (5.79%), CS-A (84.64%), and CS-C (9.58%), and the disaccharide composition of Russian sturgeon Noto-CS was CS-0 (3.06%), CS-A (86.59%), and CS-C (10.35%). Both two Noto-CSs were dominated by CS-A, the CS-A/CS-C ratio of Chinese sturgeon Noto-CS was 8.84, and that of Russian sturgeon Noto-CS was 8.37. These results were consistent with infrared spectra and $^{1}$H-NMR results. Previous studies reported that the CS-A was the major disaccharide composition of mammalian CS and avian CS. The CS-A/CS-C ratio of chick cartilage CS and porcine cartilage CS was 3.58 and 5.47, respectively [36, 42]. It suggested that CS-A content of Chinese and Russian sturgeon Noto-CS was much higher than that of terrestrial CSs.

The disaccharide composition of Cart-CS results were similar to previous reports by Gui and Im [27, 30]. They showed that the main disaccharide composition of sturgeon backbone Cart-CS was CS-A and CS-C, and the percentage of CS-C was higher than that of CS-A. Similar with the present results, Yamagata and Ototani showed that Noto-CS of sturgeon was mainly composed of CS-A [35, 36]. These

353 data suggested that the differences of disaccharide composition among sturgeon species in the same
354 tissue was not obvious, however, the disaccharide composition of Cart-CS and Noto-CS was
355 significantly different. In contrast, Wang reported the main disaccharide composition of sturgeon
356 (*Acipenser schrenckii*) Cart-CS was CS-A [29]. Also, Wu reported that approx. 15% di-sulfated
357 disaccharide CS-D was detected in the hybrid sturgeon (*A. schrenckii* × *H. dauricus*) Cart-CS [48]. The
358 reason for this discrepancy is unclear at present, and it is necessary to re-compare the disaccharide
359 composition between sturgeon species in further study.
360 In the human body, CS-A mainly exists in the platelets and brain tissues accounting for more than
361 90% of total CSs [49, 50]. Previous study reported that CS-A, but not CS-C, exhibited a strong
362 negative guidance cue to cerebellar granule neurons and modulated the axons growing in mouse brain
363 [51]. Albertini showed that CS-A could affect the metal ion-induced lipoprotein oxidation [52]. Thus,
364 sturgeon notochord has potential to be used as a novel and safe source of fish CS-A for the functional
365 foods and pharmaceutical industries.
366 **3.7. Antioxidant activity of CS**
367 The antioxidant activity of sturgeon CS was analyzed using ABTS and hydroxyl radical
368 scavenging activities and compared with shark and bovine CSs (Fig. 6). All CS samples showed free
369 radical scavenging activity in a dose-dependent manner and the activity of CS was much lower than
370 that of Vc. The ABTS radical scavenging assay (Fig. 6-A) showed that the activity of Russian sturgeon
371 CSs from the same tissue was higher than that of Chinese sturgeon CSs. The activity of Cart-CS was
372 higher than that of Noto-CS in both two sturgeons. The activity of sturgeon CS was higher than that of
373 shark CS. Bovine CS exhibited the lowest activity compared to sturgeon and shark CSs. In the
374 disaccharide analysis (in section 3.6), we demonstrated that sturgeon Cart-CS and Noto-CS were

mainly composed of CS-C and CS-A, respectively. Shark CS and bovine CS were mainly composed of CS-C and CS-A, respectively. It suggested that the ABTS radical scavenging activity of CS-C was higher than that of CS-A. This finding was different from the reported by Campo et al (2006), the in vitro antioxidant activity of CS-A was higher than that of CS-C due to its strong metal cation binding capacity [19]. Ajisaka et al. reported that the CS extracted from porcine mucosa containing a high CS-A ratio showed lower antioxidant activity than shark CS [53]. It meant that the ABTS radical scavenging activity of CS-C was not only independent of its metal cation binding capacity. The hydroxyl radical scavenging assay (Fig. 6-B) showed that the activity of all sturgeon CS was similar, but was higher than that of shark and bovine CSs. Zhou et al (2016) reported that the hydroxyl radical scavenging activity of sturgeon *(Acipenser baerii)* cartilage CS connected with its concentration [54]. The differences in the ability of CS to scavenge the two free radicals might be due to the difference in its scavenging mechanism. This was the first time to compare the antioxidant activities of sturgeon Cart-CS and Noto-CS, but the difference in activity caused by different structures was not obvious. Based on these two free radical scavenging activity results, we concluded that the antioxidant activity of sturgeon CSs was higher than that of shark and bovine CSs. More importantly, farmed Russian sturgeon CS could replace the rare Chinese sturgeon CS as a natural macromolecular antioxidant.

CS is a structurally regular linear polysaccharide chain composed of alternating disaccharide units of glucuronic acid and N-acetyl-galactosamine, modified with sulfated groups [14]. To further explore the mechanism of antioxidant activity of CS, we detected the free scavenging activity of CS building blocks, glucuronic acid (GA), acetyl-galactosamine (AG), and sodium methyl sulfate (SMS), respectively (Fig. 7). Although the ABTS scavenging activities (Fig. 7-A) of GA and AG increased with increasing concentration, the activities were weak even at high concentrations. It suggested

scavenging activity of CS was not from individual GA or AG, but from the interaction of its own structure. The hydroxyl activities (Fig. 7-B) of GA and AG increased with increasing concentration, and the activity of GA was higher than that of AG. SMS did not exhibit ABTS and hydroxyl radical scavenging activities. Some studies have reported that the sulfate and carboxylate groups had metal chelating ability, thereby exhibiting antioxidant activity [19, 55]. The results of present study indicated that the main sites for direct scavenging of hydroxyl were on the GA and AG of CS, rather than on the sulfate group of CS chain.

**3.8. The effects of CS on collagen fibril formation**

Collagen fibril formation *in vitro* was a self-assembly process from soluble collagen molecule to insoluble fibrils. The turbidity changes in the solution reflected different stages of fibril formation process [56]. In general, collagen fibril-forming process is divided into three phases: lag phase (no turbidity changes), growth phase (turbidity increasing), and plateau phase (turbidity stabilization) [27]. The effects of Noto-CS and Cart-CS on type I collagen fibril formation process were shown in Fig. 8. For both Chinese sturgeon and Russian sturgeon CSs, the addition of CS into collagen solution reduced the slope of the growth phase curve and the final turbidity value in the plateau phase. It suggested that CS inhibited the lateral aggregation of fibrils. In section 3.5, we demonstrated that CS was a polyanionic chain structure composed of disaccharide units of glucuronic acid and sulfated N-acetyl galactosamine. The negative carboxyl and sulfonic acid groups of the CS chain were both anions under neutral conditions. These anions interacted with the amino groups of basic amino acids such as lysine, hydroxylysine, histidine and arginine on the side chain of collagen through electrostatic attraction. Multiple anions on the CS chain combined with amino ions on different collagen molecules or fibrils to form steric hindrance, which was dispersed between collagen molecules or fibrils, thereby affecting the

later aggregation of fibrils. Mathews (1968) have reported that electrostatic interaction was important for polyanions on collagen aggregation [57]. More importantly, the Cart-CS addition turbidity curve entered to plateau phase faster than the Noto-CS addition turbidity curve. In section 3.6, we demonstrated that the major disaccharide component of Cart-CS was CS-C, while the major disaccharide component of Noto-CS was CS-A. It meant that the inhibition effect of CS-C on type I collagen was stronger than that of CS-A. Furthermore, it showed that the binding ability of CS-C on type I collagen was stronger than that of CS-A.

The collagen fibril morphology was shown in Fig. 9. As the turbidity curves of Chinese and Russian CS on collagen fibril formation were similar. Here, we analyzed the effect of Chinese sturgeon CS on collagen fibril morphology. A network of fibrillar structure was formed in both the non-CS and CS-added samples. The most significant differences between non-CS and CS-added samples were fibrillar morphology and diameter. As shown by the white arrows in Fig. 9 (A), in non-CS sample, coarse fibrils were assembled in parallel by many thin fibrils. Although some coarse fibrils appeared in the sample with Noto-CS added, the fibril diameters were thinner than the sample without CS. The Cart-CS added sample formed many fine fibrils with a non-uniform network structure. The fibril diameters of Cart-CS added sample were thinner than that of Noto-CS added sample. The fibril morphology results indicated that the CS reduced self-assembly of collagen molecules into coarse fibrils. This result was consistent with the turbidity curve results for collagen fibril formation. This is the first discussion of the *in vitro* interaction of sturgeon by-products derived CS and collagen. The results of this study will facilitate the development of biomimetic material forms for biomedical applications using sturgeon CS and collagen.

## 4. Conclusion

In this study, Cart-CS and Noto-CS were extracted from Chinese sturgeon and Russian sturgeon, respectively. The molecular weight of Cart-CS was higher than that of Noto-CS in both two sturgeons and the molecular weight of Chinese Cart-CS was the highest. The disaccharide composition of Cart-CS was mainly composed by CS-A and CS-C. The CS-A/CS-C ratios of Chinese sturgeon Cart-CS and Russian sturgeon Cart-CS were 0.53 and 0.68, respectively. The disaccharide composition of both Noto-CSs was mainly composed of CS-A. The CS-A/CS-C ratios of Chinese sturgeon Noto-CS and Russian sturgeon Noto-CS were 8.84 and 8.37, respectively. The structural properties of CSs in sturgeon species seems to be dependent on tissues in origin, but not on species. The antioxidant activity of sturgeon CS was higher than that of shark and bovine CSs. The present study is the first report to compare the structural properties and antioxidant activities of Noto-CS and Cart-CS in the same species with the same extraction method. Furthermore, the inhibition of Cart-CS on type I collagen self-assemble was stronger than that of Noto-CS. From these results, we conclude that the CS derived from Chinese sturgeon can be substituted by that from other available commercial sturgeons. In addition, Russian sturgeon backbone and notochord are good resource of CS-C and CS-A, respectively. Sturgeon CS is a good source of natural macromolecular antioxidants and biological biomaterials. Other functional activities of sturgeon Cart-CS and Noto-CS will be discussed in further studies.

**Acknowledgements**

This work was partially supported by key laboratory research fund open topics (LFBC1002) from Key Lab of Freshwater Biodiversity Conservation, Ministry of Agriculture and Rural Affairs of China; The discipline innovation and talent introducing program for high education institutions, the 111 project (D21012).

**Compliance with ethical standards**

**Conflicts of interest**

The authors declare that have no conflicts of interest.

**Declaration of competing interest**

The authors declare no competing financial interest.

**Authors contribution**

**Dawei Meng**: Methodology, Data curation, Writing-original draft. **Wen Li**: Methodology. **Xiaoqian Leng:** Methodology. **Yan Zhang**: Methodology. **Zhiyuan Dai:** Supervision, Fish providing. **Qiwei Wei:** Supervision, Fish providing. **Hao Du:** Supervision, Fish providing. **Yasuaki Takagi:** Methodology, Writing-review & Editing.

**References**

[1] D. Q. Wang, L. Zhong, Q. W. Wei, X. N. Gan, S. P. He, Evolution of MHC class I genes in two ancient fish, paddlefish *(Polyodon spathula)* and Chinese sturgeon *(Acipenser sinensis)*, FEBS. Letters. 584 (2010) 3331-3339.

[2] X. F. Zhou, L. Chen, J. Yang, H. Q. Wu, Chinese sturgeon needs urgent rescue, Scinece. 370 (2020) 1174-1175.

[3] J. H. Wang, Q. W. Wei, Y. C. Zou, Conservation strategies for the Chinese sturgeon, Acipenser sinensis: an overview on 30 years of practices and future needs, J. Appl. Ichthyol. 27 (2011) 176-180.

[4] H. Cao, L. Zhou, Y. Z. Zhang, Q. W. Wei, X. H. Chen, J. F. Gui, Molecular characterization of Chinese sturgeon gonadotropins and cellular distribution in pituitaries of mature and immature individuals, Mol. Cell. Endocrinol. 30 (2009) 334-342.

[5] H. Peng, Q. W. Wei, Y. Wan, J. P. Giesy, L. X. Li, J. Y. Hu, Tissue distribution and maternal transfer

485 of poly- and perfluorinated compounds in Chinese sturgeon *(Acipenser sinensis)*: implications for
486 reproductive risk, Environ. Sci. Technol. 44 (2010) 1868-1874.
487 [6] Y. H. Zhu, J. M. Wu, X. Q. Leng, H. Du, J. P. Wu, S. He, J. Luo, X. F. Liang, H. Liu, Q. W. Wei, Q.
488 S. Tan, Metabolomics and gene expressions revealed the metabolic changes of lipid and amino
489 acids and the related energetic mechanism in response to ovary development of Chinese sturgeon
490 *(Acipenser sinensis)*, PloS One. 15 (2020) 1-19.
491 [7] A. Hurvite, K. Jackson, G. Gegani, B. Levavi-Sivan, Use of endoscopy for gender and ovarian stage
492 determinations in Russian sturgeon *(Acipenser gueldenstaedtii)* grown in aquaculture,
493 Aquaculture. 270 (2007) 158-166.
494 [8] Y. W. Chen, W. Q. Cai, Y. G. Shi, X. P. Dong, F. Bai, S. K. Shen, R. Jiao, X. Y. Zhang, X. Zhu,
495 Effects of different salt concentrations and vacuum packaging on the shelf stability of Russian
496 sturgeon *(Acipenser gueldenstaedti)* stored at 4 °C. Food Control. 109 (2020) 106865.
497 [9] D. W. Meng, H. Tanaka, T. Kobayashi, H. Hatayama, X. Zhang, K. Ura, S. Yunoki, Y. Takagi, The
498 effect of alkaline pretreatment on the biochemical characteristics and fibril-forming abilities of
499 types I and II collagen extracted from bester sturgeon by-products, Int. J. Biol. Macromol. 131
500 (2019) 572–580.
501 [10] K. Shionoya, T. Suzuki, M. Takada, K. Sato, S. Onishi, N. Dohmae, K. Nishino, T. Wada, R. J.
502 Linhardt, T. Toida, K. Higashi, Comprehensive analysis of chondroitin sulfate and aggrecan in the
503 head cartilage of bony fishes: Identification of proteoglycans in the head cartilage of sturgeon, Int.
504 J. Biol. Macromol. 208 (2022) 333-342.
505 [11] A. N. Ivankin, S. E. Vasyukov, V. P. Panov, Production, properties, and use of chondroitin sulfates
506 (survey), Pharm. Chem. J. 19 (1985) 192-202.

[12] M. M. Fuster, J. D. Esko, The sweet and sour of cancer: glycans as novel therapeutic targets, Nature. 5 (2005) 526-542.

[13] N. S. Gandhi, R. L. Mancera, The structure of glycosaminoglycans and their interactions with proteins, Chem. Biol. Drug. Des. 72 (2008) 455-482.

[14] S. Yamada, K. Sugahara, Potential therapeutic application of chondroitin sulfate/dermatan sulfate, Curr. Drug. Discov. Technol. 5 (2009) 289-301.

[15] N. Volpi, Quality of different chondroitin sulfate preparations in relation to their therapeutic activity, J. Pharm. Pharmacol. 61 (2009) 1270-1280.

[16] Y. Sano, Antiviral activity of chondroitin sulfate against infection by tobacco mosaic virus, Carbohyd. Polym. 33 (1997) 125-129.

[17] M. B. Mansour, R. Balti, V. Ollivier, H. B. Jannet, F. Chaubet, R. M. Maaroufi, Characterization and anticoagulant activity of a fucosylated chondroitin sulfate with unusually procoagulant effect from sea cucumber, Carbohyd. Polym. 174 (2017) 760-771.

[18] R. Lan, Y. Li, R. Shen, R. Yu, L. H. Jing, S. S. Guo, Preparation of low-molecular-weight chondroitin sulfates by complex enzyme hydrolysis and their antioxidant activities. Carbohyd. Polym. 241 (2020) 116302.

[19] G. M. Campo, A. Avenoso, S. Campo, A. M. Ferlazzo, A. B. T. A. Calatroni, Antioxidant activity of chondroitin sulfate. chondroitin sulfate: structure, role and pharmacological activity, Advances in Pharmacology. 53 (2006) 417-431.

[20] P. A. S. Mourão, Distribution of chondroitin 4-sulfate and chondroitin 6-sulfate in human articular and growth cartilage, Arthritis. Rheum. 31 (1988) 1028-1033.

[21] J. Rachmilewitz, M. L. Tykocinski, Differential effects of chondroitin sulfates A and B on

monocyte and B-Cell activation: evidence for B-Cell activation via a CD44-dependent pathway, Blood. 92 (1998) 223-229.

[22] K. Stuart, A. Panitch, Characterization of gels composed of blends of collagen I, collagen III, and chondroitin sulfate, Biomacromolecules. 10 (2009) 25-31.

[23] A. Jongjareonrak, S. Benjakul, W. Visessanguan, T. Nagai, M. Tanaka, Isolation and characterisation of acid and pepsin-solubilized collagens from the skin of brownstripe red snapper *(Lutjanus vitta)*, Food. Chem. 93 (2005) 475–484.

[24] F. Maccari, F. Galeotti, N. Volpi, Isolation and structural characterization of chondroitin sulfate from bony fishes, Carbohyd. Polym. 129 (2015) 143-147.

[25] W. Li, T. Kobayashi, D. W. Meng, N. Miyamoto, N. Tsutsumi, K. Ura, Y. Takagi, Free radical scavenging activity of type II collagen peptides and chondroitin sulfate oligosaccharides from by-products of mottled skate processing, Food. Biosci. 41 (2021) 100991.

[26] X. Pan, Y. Zhao, F. Hu, B. Wang, Preparation and identification of antioxidant peptides from protein hydrolysate of skate *(Raja porosa)* cartilage. J. Funct. Foods. 25 (2016) 220-230.

[27] D. W. Meng, W. Li, K. Ura, Y. Takagi, Effects of phosphate ion concentration on in-vitro fibrillogenesis of sturgeon type I collagen, Int. J. Biol. Macromol.148 (2020) 182-191.

[28] M. Gui, J. Y. Song, L. Zhang, S. Wang, R. Y. Wu, C. W. Ma, P. L. Li, Chemical characteristics and antithrombotic effect of chondroitin sulfates from sturgeon skull and sturgeon backbone, Carbohyd. Polym. 123 (2015) 454-460.

[29] T. Wang, S. L. Zhang, S. Y. Ren, X. Zhang, F. Yang, Y. Chen, B. Wang, Structural characterization and proliferation activity of chondroitin sulfate from the sturgeon, *Acipenser schrenckii*, Int. J. Biol. Macromol. 164 (2020) 3005-3011.

[30] A. R. Im, Y. Park, Y. S. Kim, Isolation and Characterization of Chondroitin Sulfates from Sturgeon *(Acipenser sinensis)* and Their Effects on Growth of Fibroblasts, Biol. Pharm. Bull. 33 (2010) 1268-1273.

[31] F. Krichen, H. Bougatef, N. Sayari, F. Capitani, I. B. Amor, I. Koubaa, F. Maccari, V. Mantovani, F. Galeotti, N. Volpi, A. Bougate, Isolation, purification and structural characterestics of chondroitin sulfate from smooth hound cartilage: *In vitro* anticoagulant and antiproliferative properties, Carbohyd. Polym. 197 (2018) 451-459.

[32] L. Yang, Y. H. Wang, S. Yang, Z. H. Lv, Separation, purification, structures and anticoagulant activities of fucosylated chondroitin sulfates from Holothuria scabra, Int. J. Biol. Macromol. 108 (2018) 710-718.

[33] M. Flower, C. Grobetein, Interconvertibility of induced morphogenetic responses of mouse embryonic somites to notochord and ventral spinal cord, Dev. Biol. 15 (1967) 193-205.

[34] D. L. Stemple, Structure and function of the notochord: an essential organ for chordate development, Development. 132 (2005) 2503-2512.

[35] M. Yamagata, K. Kimata, Y. Oike, K. Tani, N. Maeda, K. Yoshia, Y. Shimomura, M. Yoneda, S. Suzuki, A Monoclonal Antibody That Specifically Recognizes a Glucuronic Acid 2-Sulfate-containing Determinant in Intact Chondroitin Sulfate Chain, J. Biol. Chem. 262 (1987) 4146-4152.

[36] N. Ototani, N. Sato, Z. Yosizawa, High performance liquid chromatography of unsaturated disaccharides produced from chondroitin sulfates by chondroitinase, J. Biochem. 85 (1979) 1383-1385.

[37] P. Bronzi, M. Chebanov, J. T. Michaels, Q. W. Wei, H. Rosenthal, J. Gessner, Sturgeon meat and caviar production: Global update 2017, J. Appl. Ichthyol. 35 (2019) 257-266.

573 [38] K. Y. Wang, F. Bai, X. D. Zhou, J. L. Wang, Y. J. Li, H. Xu, R. C. Gao, H. H. Wu, K. Liu, Y. H.
574 Zhao, Characterization of chondroitin sulfates isolated from large hybrid sturgeon cartilage and
575 their gastroprotective activity against ethanol-induced gastric ulcers. Food. Chem. 363 (2021)
576 130436.
577 [39] W. M. Zhu, Y. Ji, Y. Wang, D. He, Y. S. Yan, N. Su, C. Zhang, X. H. Xing, Structural
578 characterization and in vitro antioxidant activities of chondroitin sulfate purified from Andrias
579 davidianus cartilage, Carbohyd. Polym. 196 (2018) 398-404.
580 [40] F. Krichen, H. Bougatef, F. Capitani, I. B. Amor, I. Koubaa, J. Gargouri, F. Maccari, V. Mantovani,
581 F. Galeotti, N. Volpi, A. Bougatef, Purification and structural elucidation of chondroitin
582 sulfate/dermatan sulfate from Atlantic bluefin tuna *(Thunnus thynnus)* skins and their
583 anticoagulant and ACE inhibitory activities, R. S. C. 8 (2018) 37965-37975.
584 [41] W. Garnjanagoonchorn, L. Wongekalak, A. Engkagul, Determination of chondroitin sulfate from
585 different sources of cartilage, Chem. Eng. Process. 46 (2007) 465-471.
586 [42] M. Foot, M. Mulholland, Classification of chondroitin sulfate A, chondroitin sulfate C,
587 glucosamine hydrochloride and glucosamine 6 sulfate using chemometric techniques, J.
588 Pharmaceut. Biomed. 38 (2005) 397-407.
589 [43] C. Zhou, S. Mi, J. Li, J. Gao, X. H. Wang, Y. X. Sang, Purification, characterisation and
590 antioxidant activities of chondroitin sulphate extracted from *Raja porosa* cartilage. Carbohyd.
591 Polym. 241 (2020) 116306.
592 [44] Q. S. Shen, C. H. Zhang, W. Jia, X. J. Qin, Z. K. Cui, H. Z. Mo, A. Richel, Co-production of
593 chondroitin sulfate and peptide from liquefied chicken sternal cartilage by hot-pressure. Carbohyd.
594 Polym. 222 (2019) 115015.

595 [45] A. Mucci, L. Schenetti, N. Volpi, 1H and 13C nuclear magnetic resonance identification and
596 characterization of components of chondroitin sulfates of various origin, Carbohyd. Polym. 41
597 (2000) 37-45.
598 [46] M. Lopez-Alvarez, P. Gonzalez, J. Serra, J. Fraguas, J. Valcarcel, J. A. Vazquez, Chondroitin
599 sulfate and hydroxyapatite from Prionace glauca shark jaw: physicochemical and structural
600 characterization, Int. J. Biol. Macromol. 156 (2020) 329-339.
601 [47] T. Toida, H. Toyoda, T. Imanari, High-resolution proton nuclear magnetic resonance studies on
602 chondroitin sulfates, Anal. Sci. 9 (1993) 53-58.
603 [48] R. Y. Wu, P. L. Li, Y. Wang, N. Su, M. Y. Xiao, X. J. Li, N. Shang, Structural analysis and anti-
604 cancer activity of low-molecular-weight chondroitin sulfate from hybrid sturgeon cartilage.
605 Carbohyd. Polym. 275 (2022) 118700.
606 [49] S. Davidson, L. Gilead, M. Amira, H. Ginsburg, E. Razin, Synthesis of chondroitin sulfate D and
607 heparin proteoglycans in murine lymph node-derived mast cells: the dependence on fibroblasts, J.
608 Biol. Chem. 265 (1990) 12324-12330.
609 [50] H. B. Nader, Characterization of a heparan sulfate and a peculiar chondroitin 4-sulfate
610 proteoglycan from platelets: inhibition of the aggregation process by platelet chondroitin sulfate
611 proteoglycan, J. Biol. Chem. 266 (1991) 10518-10523.
612 [51] H. Wang, Y. Katagiri, T. E. McCann, E. Unsworth, P. Goldsmith, Z. X. Yu, L. Santiago, E. M.
613 Mills, Y. Wang, A. J. Symes, H. M. Geller, Chondroitin-4-sulfation negatively regulates axonal
614 guidance and growth, J. Cell. Sci. 121 (2008) 3083-3091.
615 [52] R. Albertini, G. D. Luca, A. Passi, R. Moratti, P. M. Abuja, Chondroitin-4-sulfate protects high-
616 density lipoprotein against copper-dependent oxidation, Arch. Biochem. Biophys. 365 (1999) 143-

149.

[53] K. Ajisaka, Y. Oyanagi, T. Miyazaki, Y. Suzuki, Effect of the chelation of metal cation on the antioxidant activity of chondroitin sulfates, Biosci. Biotech. Bioch. 80 (2016) 1179-1185.

[54] W. J. Zhou, S. X. Hao, L. H. Li, Y. Y. Wu, Y. Wei, J. W. Cen, Research of purification and antioxidant function of the chondroitin sulfate extracted from sturgeon, Medicine and biopharmaceutical, 1 (2016) 1253-1260.

[55] G. M. Campo, A. Avenoso, S. Campo, A. M. Ferlazzo, A. Calatroni, Chondroitin sulphate: Antioxidant properties and beneficial effects, Mini-rev. Med. Chem. 6 (2006) 1311-1320.

[56] X. Zhang, M. Ookawa, Y. K. Tan, K. Ura, S. Adachi, Y. Takagi, Biochemical characterisation and assessment of fibril-forming ability of collagens extracted from Bester sturgeon Huso huso × Acipenser ruthenus, Food. Chem. 160 (2014) 305-312.

[57] M. B. Mathews, L. Decker, The effect of acid mucopolysaccharides and acid mucopolysaccharide-proteins on fibril formation from collagen solutions, Biochem. J. 109 (1968) 517-526.

Fig. 1. GPC-MALLS chromatogram of sturgeon CS. A: Noto-CS of Chinese sturgeon; B: Cart-CS of Chinese sturgeon; C: Noto-CS of Russian sturgeon; D: Cart-CS of Russian sturgeon.

Fig. 2. UV spectra of sturgeon CS. A-1: Cart-CS of Chinese sturgeon; A-2: Noto-CS of Chinese sturgeon; B-1: Cart-CS of Russian sturgeon; B-2: Noto-CS of Russian sturgeon.

Fig. 3. FTIR spectra of sturgeon CS. A-1: Cart-CS of Chinese sturgeon; A-2: Noto-CS of Chinese sturgeon; B-1: Cart-CS of Russian sturgeon; B-2: Noto-CS of Russian sturgeon.

Fig. 4. $^{1}$H-NMR spectroscopy of sturgeon CS. A-1: Cart-CS of Chinese sturgeon; A-2: Cart-CS of Russian sturgeon; B-1: Noto-CS of Chinese sturgeon; B-2: Noto-CS of Russian sturgeon.

639 Fig. 5. Disaccharide analysis of Cart-CS of Chinese sturgeon (A); Noto-CS of Chinese sturgeon (B);

640 Cart-CS of Russian sturgeon (C); Noto-CS of Russian sturgeon (D); Cart-CS of Shark (E); Cart-CS of

641 Bovine (F).

642 Fig. 6. Antioxidant activity of Cart-CS and Noto-CS, (A) ABTS scavenging activity; (B) Hydroxyl

643 scavenging activity. Values are mean ± SD of triplicate measurements.

644 Fig. 7. Antioxidant activity of glucuronic acid (GA), N-acetyl-galactosamine (AG), and sodium methyl

645 sulfate (SMS). (A) ABTS scavenging activity; (B) Hydroxyl scavenging activity. Values are mean ± SD

646 of triplicate measurements.

647 Fig. 8. The effect of CS on type I fibril formation. A: Chinese sturgeon CS; B: Russian sturgeon CS.

648 Fig. 9. The effect of CS on type I collagen fibril morphology. Scale bar: 1 μm. A: Non-CS sample; B:

649 Noto-CS added sample; C: Cart-CS added sample.

**Highlights**

- Two kinds of CS were obtained from *Acipenser sinensis* and *Acipenser gueldenstaedti*.
- The average molecular weight of cartilage CS was higher than that of notochord CS.
- Cartilage CS was mainly composed by CS-C; Notochord CS was almost composed by CS-A.
- The inhibition of CS-C on collagen fibril-forming was higher than that of CS-A.
- The CS from *Acipenser sinensis* can be substituted by that from commercial sturgeon.

*Clarify the structural properties of CSs from Chinese sturgeon and Russian sturgeon*

***Chinese sturgeon (Acipenser sinensis)***

***Russian sturgeon (Acipenser gueldenstaedti)***

**Backbone cartilage**

**Notochord**

**Chinese sturgeon CS**
- **Cartilage CS**
- **Notochord CS**

**Russian sturgeon CS**
- **Cartilage CS**
- **Notochord CS**

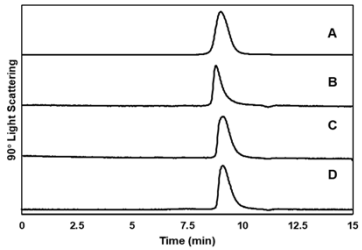


**Molecular weight analysis**

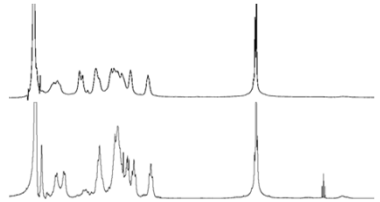

**$^{1}$H-NMR analysis**

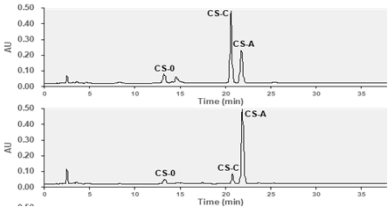


**Disaccharide composition**

Fig.1

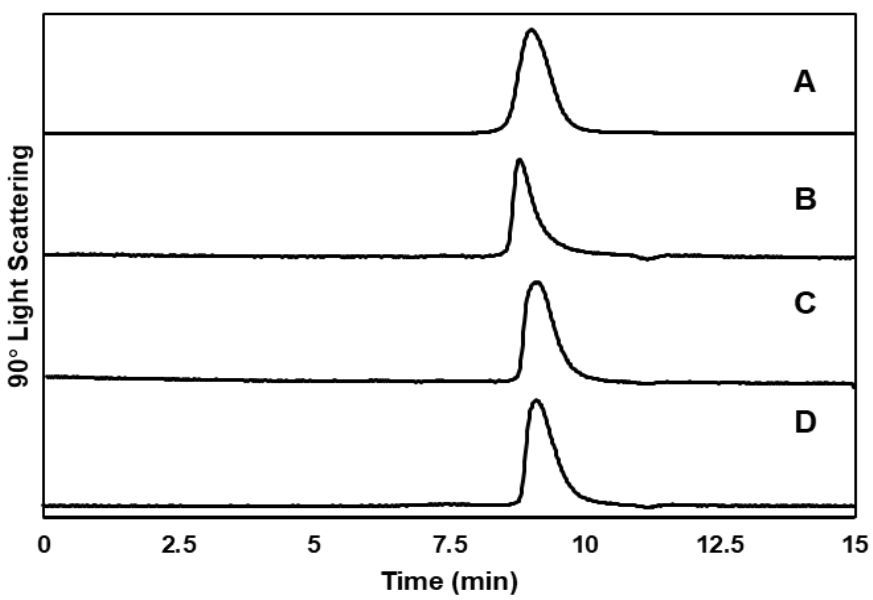

Fig.2

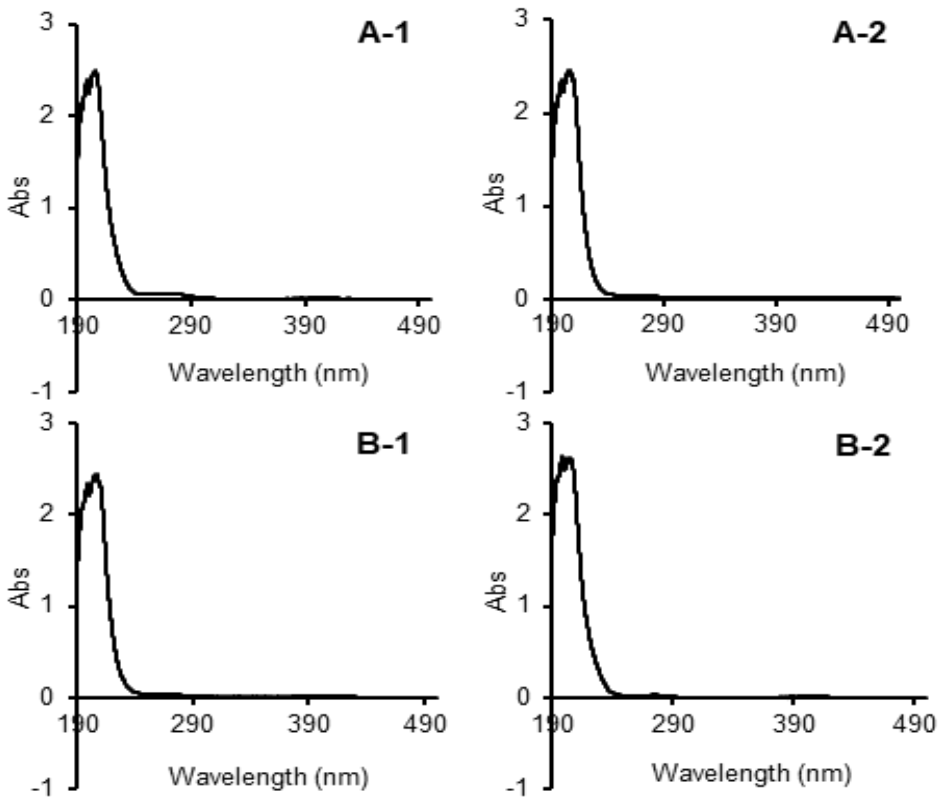

Fig.3

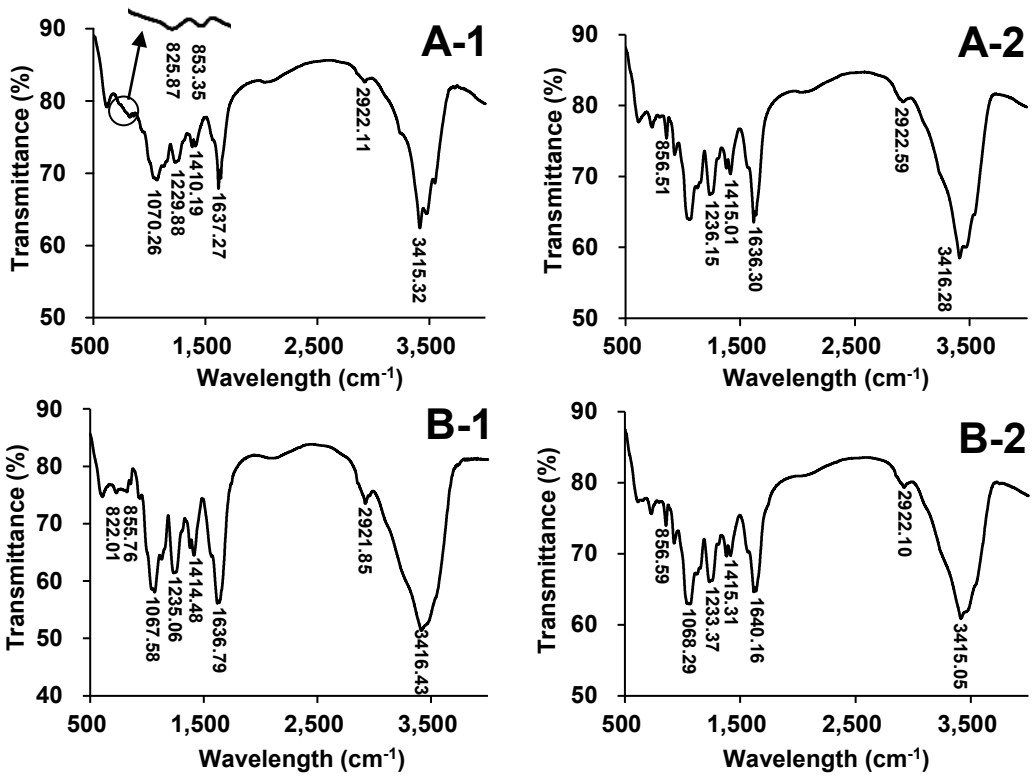
A-1
Transmittance (%)
Wavelength (cm-1)
853.35
825.87
1410.19
1229.88
1070.26
1637.27
2922.11
3415.32
A-2
856.51
1415.01
1236.15
1636.30
2922.59
3416.28
B-1
855.76
822.01
1067.58
1235.06
1414.48
1636.79
2921.85
3416.43
B-2
856.59
1068.29
1233.37
1415.31
1640.16
2922.10
3415.05

Fig.4

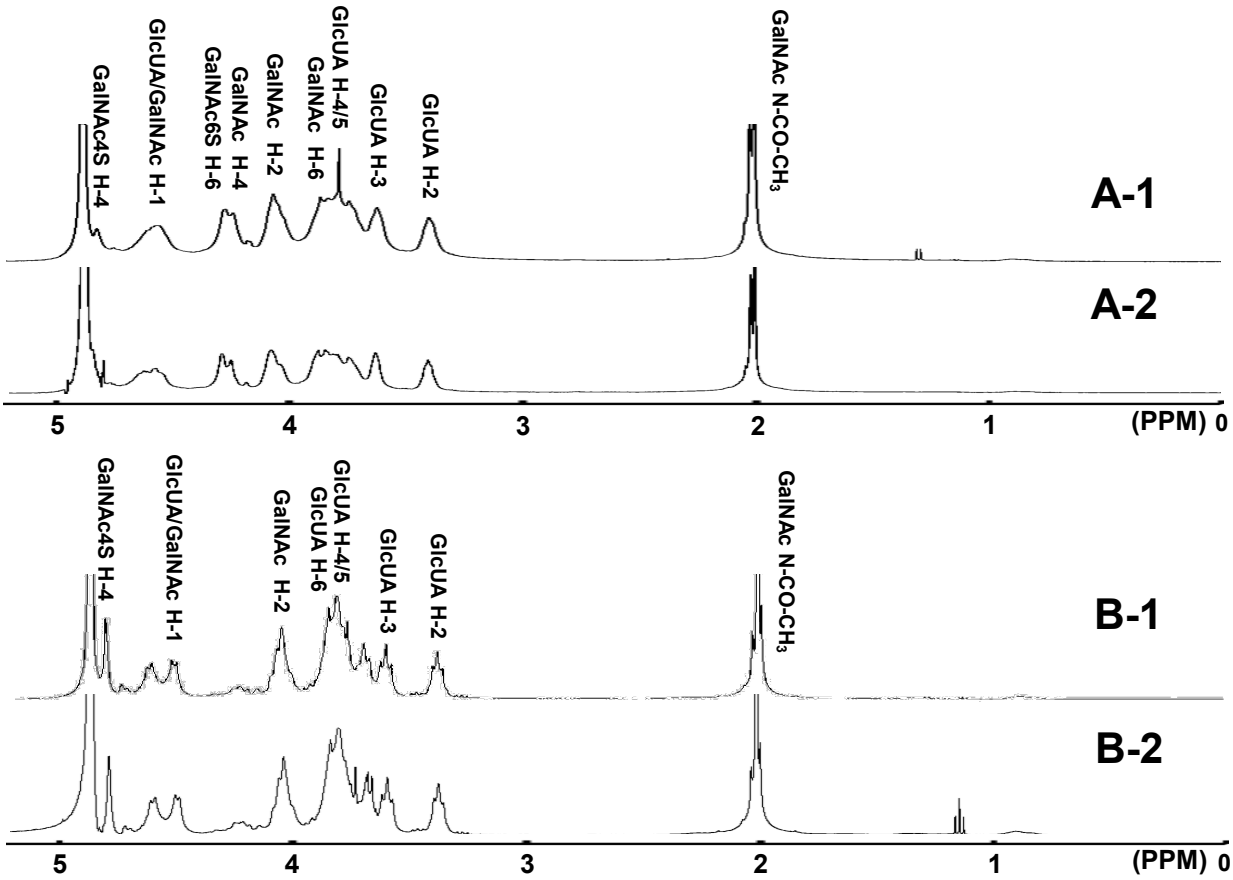
GalNAc4S H-4
GlcUA/GalNAc H-1
GalNAc6S H-6
GalNAc H-4
GalNAc H-2
GlcUA H-4/5
GalNAc H-6
GlcUA H-3
GlcUA H-2
GalNAc N-CO-CH3
A-1
A-2
5
4
3
2
1
(PPM) 0
GalNAc4S H-4
GlcUA/GalNAc H-1
GalNAc H-2
GlcUA H-4/5
GlcUA H-6
GlcUA H-3
GlcUA H-2
GalNAc N-CO-CH3
B-1
B-2
5
4
3
2
1
(PPM) 0

Fig.5

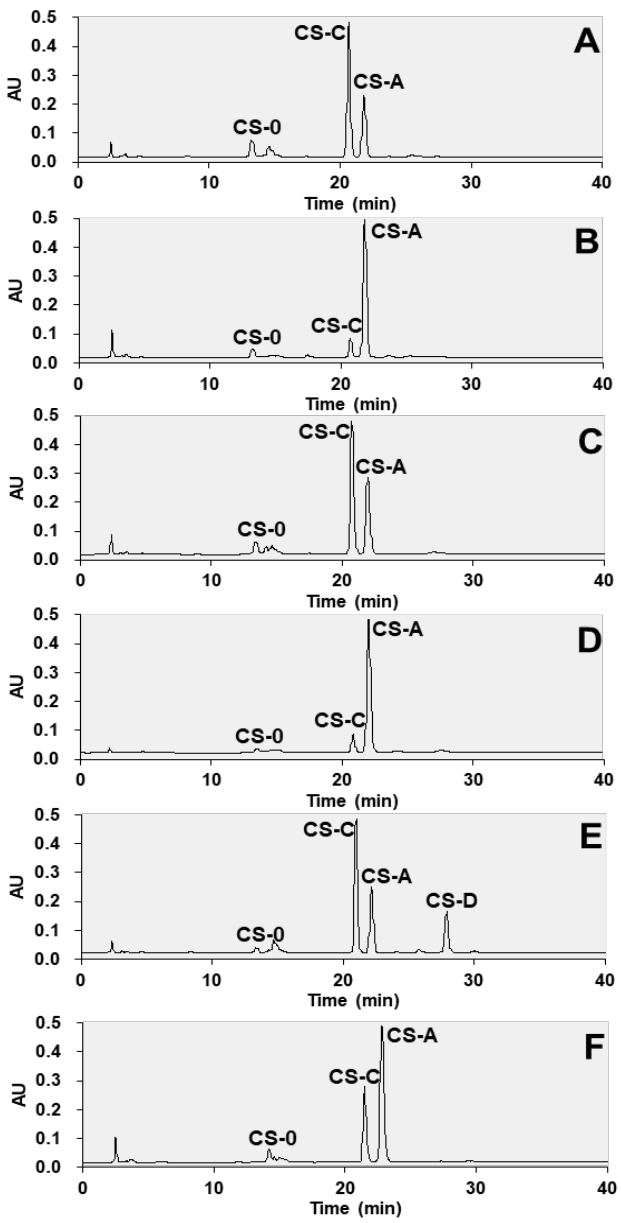
A
CS-C
CS-A
CS-0
B
CS-A
CS-C
CS-0
C
CS-C
CS-A
CS-0
D
CS-A
CS-C
CS-0
E
CS-C
CS-A
CS-D
CS-0
F
CS-A
CS-C
CS-0
AU
Time (min)

Fig.6

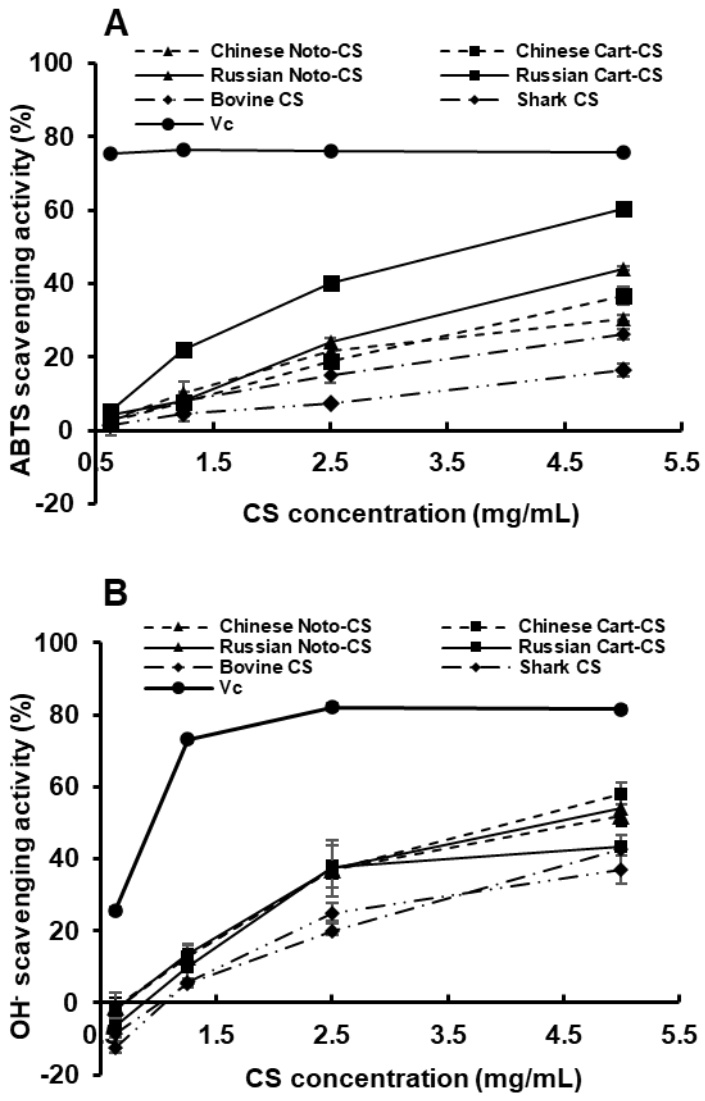
A
Chinese Noto-CS
Chinese Cart-CS
Russian Noto-CS
Russian Cart-CS
Bovine CS
Shark CS
Vc
ABTS scavenging activity (%)
100
80
60
40
20
0
-20
0
0.5
1.5
2.5
3.5
4.5
5.5
CS concentration (mg/mL)
B
Chinese Noto-CS
Chinese Cart-CS
Russian Noto-CS
Russian Cart-CS
Bovine CS
Shark CS
Vc
OH· scavenging activity (%)
100
80
60
40
20
0
-20
0
1.5
2.5
3.5
4.5
5.5
CS concentration (mg/mL)

Fig.7

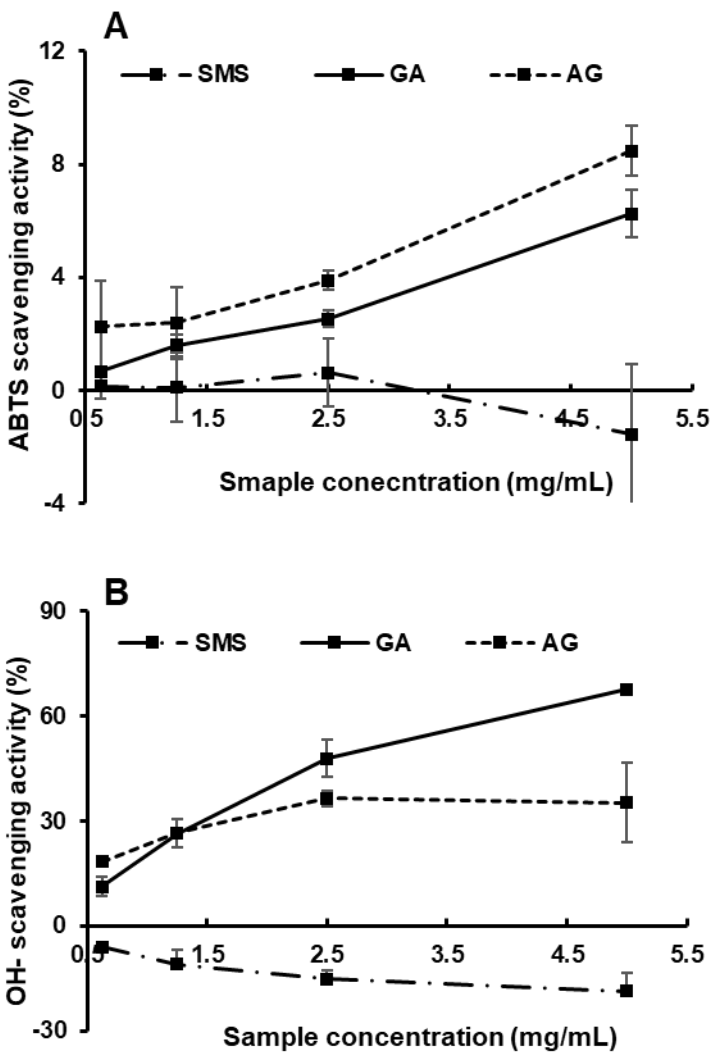
A
SMS
GA
AG
ABTS scavenging activity (%)
12
8
4
0
-4
0.5
1.5
2.5
3.5
4.5
5.5
Smaple conecntration (mg/mL)
B
SMS
GA
AG
OH- scavenging activity (%)
90
60
30
0
-30
0.5
1.5
2.5
3.5
4.5
5.5
Sample concentration (mg/mL)

Fig.8

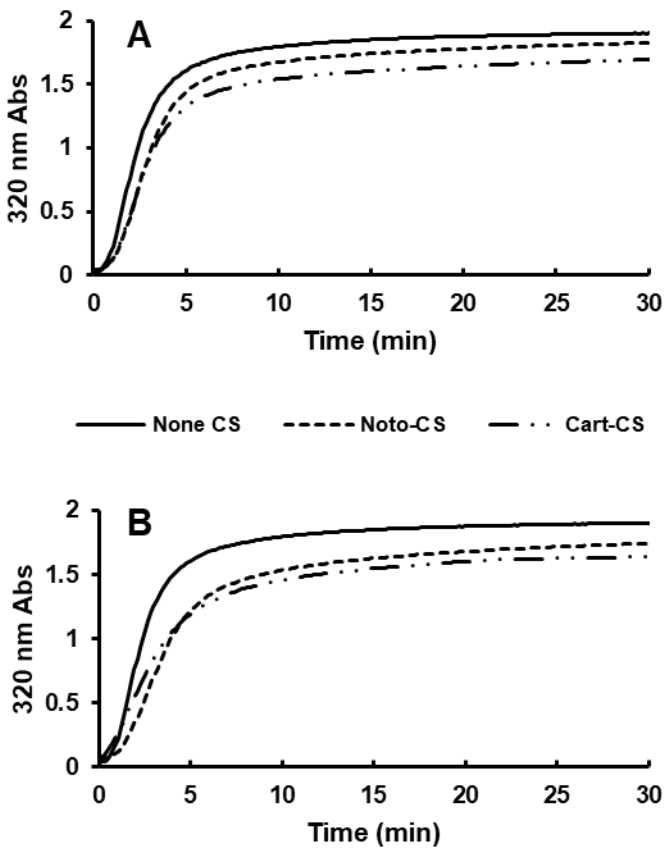
A
320 nm Abs
2
1.5
1
0.5
0
0
5
10
15
20
25
30
Time (min)
None CS
Noto-CS
Cart-CS
B
320 nm Abs
2
1.5
1
0.5
0
0
5
10
15
20
25
30
Time (min)

Fig.9